World Cancer Research Journal WCRJ 2021; 8: e2127

NILOTINIB REPOSITIONING IN CANCERS IMPLYING CX43 TUMORIGENESIS PROCESS

S. BERRAHOUI[1], S. CHERRAK[1], M. SAKER[1], H. MERZOUK[1], M. DALI-SAHI[2]

[1]Department of Biology, Faculty of Natural Sciences of life/Earth and Universe, Abou Bekr Belkaid University, Laboratory of Physiology, Pathophysiology and Biochemistry of Nutrition, Tlemcen, Algeria
[2]Department of Biology, Faculty of Natural Sciences of life/Earth and Universe, Abou Bekr Belkaid University, Laboratory of Analytical Chemistry and Electrochemistry, Tlemcen, Algeria

Abstract – *Objective:* *Among the 21 human connexins, the ubiquitous protein Cx43 is the most abundant in many cell types. It is also associated with the tumorigenic process and the formation of metastases in several types of common cancers such as breast and colorectal cancers. Therefore, it constitutes an interesting therapeutic target in the fight against cancer. This study aims to search for drugs that could potentially interact with the Cx43 C-ter among the ones approved by the FDA.*

Materials and Methods: *By molecular modeling, we selected four molecules among 1615 (Lumacaftor, Lomapitapide, Ponatinb and Nilotinib). We analyzed their interaction with Cx43 by molecular docking and molecular dynamics simulation.*

Results: *The analysis of data allowed to highlight Nilotinib as the molecule that can best target Cx43. Indeed, although the four molecules showed strong binding energies, probably due to the hydrophobic molecular interactions with the C-ter of Cx43, only Nilotinib remains stable during the 100 ns of simulation with 2-4 hydrogen bonds.*

Conclusions: *All the molecules mentioned could play a non-negligible role in Cx43-mediated cancers. However, Nilotinib appears to be an optimal candidate in this context.*

KEYWORDS: *Cx43, Cancer, Drug repurposing, Molecular docking, MD simulation.*

INTRODUCTION

Connexin 43 (Cx43) is a ubiquitous transmembrane protein abundant in several tissues and cell types including the heart, the brain, the epidermis[1-3]. It belongs to a family of 21 isoforms that can combine into a hexameric structure called the hemicanal or connexon. Connexons of adjacent cells can form the gap junction establishing a "cell to cell" channel which allows molecules transfer of size below 1 kDa from one cell to the other, some of which being involved in intercellular signaling or electric coupling[4-6].

Cx43 is more and more being studied in tumor contexts. Indeed, it has been observed that the expression of Cx43 is correlated with the proliferation and migration of tumor cells. Numerous studies on cancer have shown its involvement in the development and progression of this pathology. Connexins are involved in the regulation of tumor proliferation, apoptosis and metastasis[7-11]. Their expression's deregulation of is associated with carcinogenesis of the lung, breast, ovary, prostate, liver, colon, colorectum, pancreas, brain, and skin[9,12-21]. In the early stages of cancer, Cx43 expression decreases in several types of cancer with loss of junctional communication[22] while its expression increases in tumors able of metastasizing. This is the case with melanoma cells, prostate tumors, bone and breast cancers. Indeed, Cx43

Corresponding Author: Berrahoui Samira, PhD; e-mail: s_berrahoui@yahoo.fr

plays a crucial role in the capacity for extravasation and colonization of tissues[16-18].

Furthermore, it was observed that mutations at the C-terminus of Cx43 (Cx43 C-ter) are associated with invasive forms of colorectal cancer and breast cancer, which would lead to aberrations on the localization of Cx43[12,14]. Alternately, Cx43 C-terminus can be expressed alone in the nucleus of different cell types. This nuclear localization allows Cx43 to regulate the expression of genes including those encoding miRNAs that play a role in the proliferation of breast cancer cells[19]. In addition, Cx43 is found in the stroma during the progression of breast cancer, allowing the regulation of invasion and metastasis through interactions between tumor cells and the stroma[18].

Due to all these observations, connexins and in particular Cx43, have emerged as ideal therapeutic targets in the treatment of cancer[18,23]. Blockade of Cx43 and Cx43 gap junctions may be a relevant strategy in cancer treatment, since gain in junctional communication and re-expression of Cx43 in advanced stages of cancer stimulate extravasation and metastasis. The objective of this study is to provide drug candidates targeting Cx43 C-ter in a tumor context, by an *in silico* approach.

MATERIALS AND METHODS

The structure of the Cx43 C-terminal domain bound to tubulin (PDB id: 2LL2) was retrieved from the protein data bank site **(**www.rcsb.org**)**.

The study used the section of small-molecules in the DrugBank database (https://zinc.docking.org) to obtain all FDA-approved drugs[24]. Non-unique structures were removed during the process and 1615 compounds were selected.

Virtual screening

The study used the Pyrx tool for virtual screening[25,26]. The Pyrx tool generated input pdbqt files for Autodock Vina and minimization steps. Finally, to screen the chosen compounds against the target, the study implemented AutoDock Vina for drug discovery. A total of the top eight poses were retained from the docking run. The 2D interactions were realized in Biovia Discovery Studio.

Molecular dynamics simulation

For further evaluations, the most interesting drugs were chosen for molecular dynamics (MD) simulation. MD simulations were directed using the GROMACS 5.1.5 package[27]. The CHARMM 36 force field was used for the complexes. The study used the SWISSPARAM server for the preparation of the coordinates and topology of ligands. The study applied appropriate amounts of chloride ions and sodium to all simulation boxes to neutralize the system. Periodic Boundary Condition (PBC) was applied along every simulation box axis, and the SP3 water model was also utilized for system solvation[28] in each simulation system. MD simulations were done through a short-range electrostatic interaction as well as a 1.2 nm distance cut off for the van der Waals interaction. The Particle Mesh Ewald (PME) algorithm calculated the long-range electrostatic interaction. The steepest descent algorithm fulfilled the energy minimization of all systems, and then the NVT ensemble for 500 ps equilibrated all the systems. Then, the NPT ensemble progressively directed the equilibration of each system and the Nose-Hoover algorithm temperature[28, 29] was preserved at a temperature of 310 K. During the NPT equilibration, the Parrinello-Rahman barostat[30] maintained the pressures at 1 bar. The MD simulation was completed for the complexes in 100 ns.

RESULTS

Molecular docking

The structure of the Cx43 C-terminal domain bound to tubulin (PDB id: 2LL2) was retrieved from the Protein Data Bank, and molecular docking was realized against FDA approved molecules.

The receptor corresponds to the K26D peptide, a 26 amino acid peptide extending from K234 to D259 of the C terminal extremity of Cx43, and able of interacting with tubulin / microtubules, as demonstrated by Nuclear Magnetic Resonance (NMR) experiments[31] (Figure 1).

The retained compounds are represented in Table 1.

The four selected molecules belong to different classes of drugs. They were selected to be repositioned, on the basis of their strong binding energy, and also their availability on the Algerian market. In addition, these molecules have no major adverse effects. The Lumacaftor (Vertex pharmaceuticals, Dublin, Ireland), is used in the treatment of cystic fibrosis, for patients homozygous for the Phe deletion at position 508 of the CFTR (Cystic fibrosis transmembrane conductance regulator) receptor. This benzoic acid is used in combination with Ivacaftor and acts by improving the transport of CFTR proteins to the cell membrane[32-34].

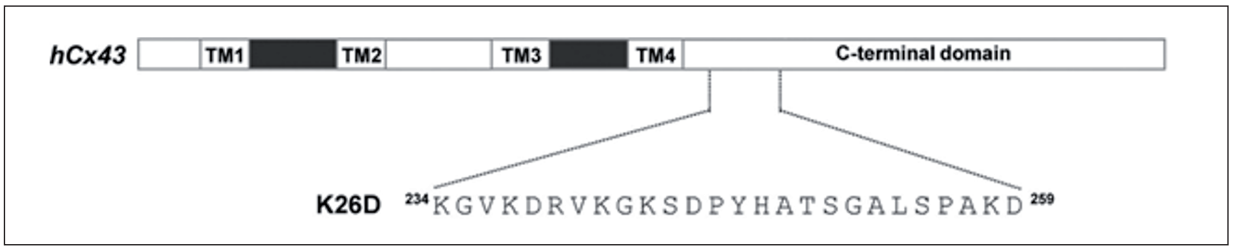

Fig. 1. Schematic representation of the human Cx43 and the K26D peptide, derived from the Cx43 tubulin binding domain as described by Saidi Brikci-Nigassa et al[31].

Lomitapide (Amryt pharmaceuticals DAC, Dublin, Ireland) is a microsomal triglyceride transfer protein inhibitor used in homozygous patients with familial hypercholesterolemia[35]. Although widely used to treat hypercholesterolemia, Lomitapide was recently shown to exhibit anti-SARS-CoV-2 activity on traditional cytopathic effect (CPE) antiviral tests (score = - 9.96 kcal / mol). In addition, Lomitapide has also been predicted to inhibit the Spike protein with a docking score of -9.26 kcal / mol, suggesting multi-target potential[36]. This compound belongs to the class of organic compounds called fluorenes[35]. Lomitapide is also part of the benzamides, fluorenes and piperidines classes[35, 37].

As for Ponatinib (Incyte biosciences distribution BV, Amsterdam, Netherlands) and Nilotinib (Novartis Europharm, Dublin, Ireland), both belong to the class of tyrosine kinase inhibitors, and both are used in the treatment of chronic myeloid leukemia[38-40]. Ponatinib is commonly indicated for the treatment of CML, in each phase of the disease resistant to Dasatinib and Nilotinib[41,42]. Several trials have shown that this drug has inhibitory activity against BCR-ABL1 kinase and several ABL1 mutations. Also known as AP24534, this benzamide can target many tyrosine kinases involved in cancers other than CML (chronic myeloid leukemia) and acute lymphocytic leukemia (ALL), including liver cancer, glioblastoma, thyroid carcinoma, and gastrointestinal stromal tumors[43]. However, it should be noted that this drug is associated with serious and dose-dependent cardiovascular risks[41,42].

A phase I clinical trial in 2006, showed that Nilotinib, also known as AMN107, was relatively safe and offered significant therapeutic benefits in cases of CML that were shown to be resistant to Imatinib (Gleevec) treatment, another tyrosine kinase inhibitor used as a first-line treatment for CML[38,44,45]. Chemically, it is an aminopyrimidine derivative, which reduces the rate of BCL-ABL transcription (≤ 10% in 3 months) as well as the risk of transformation to advanced stages of CML. However, Nilotinib should be used with caution in patients with cardiovascular risks[45]. At low doses, Nilotinib penetrates the blood-brain barrier leading to oxidative stress reduction and protection of neurons, it also increases dopamine levels and improves cognitive and motor results in models of Parkinson's and Alzheimer's disease[44]. Interactions occurring between the peptide amino acids and the retained compounds, were further determined using Discovery studio visualizer. Results show that compounds that undertake bonds with the highest strength usually bind to Val7, His15, Ala16 and Lys25 (Figure 2).

Figure 2 also reveals that all compounds show high hydrophobic interactions with Cx43 C-terminal domain amino acids, which probably contribute to the high energy observed scores. This is partly in relation with the aromatic rings in the structure of the studied compounds.

TABLE 1. Retained compounds after docking analysis.

Ligands	*Zinc Code*	*ΔG* (kcal/ml)*	*Molecular weight (g/mol)*
Lumacaftor	64033452	-8.8	452.4
Nilotinib	6716957	-8.7	529.5
Ponatinib	36701290	-8.5	532.6
Lomitapide	27990463	-8.2	693.7

*ΔG: Gibbs free energy.
*The codes vary for the same molecule from one database to another. The zinc code corresponds to a unique entry of the selected molecules in the site used (https://zinc.docking.org).

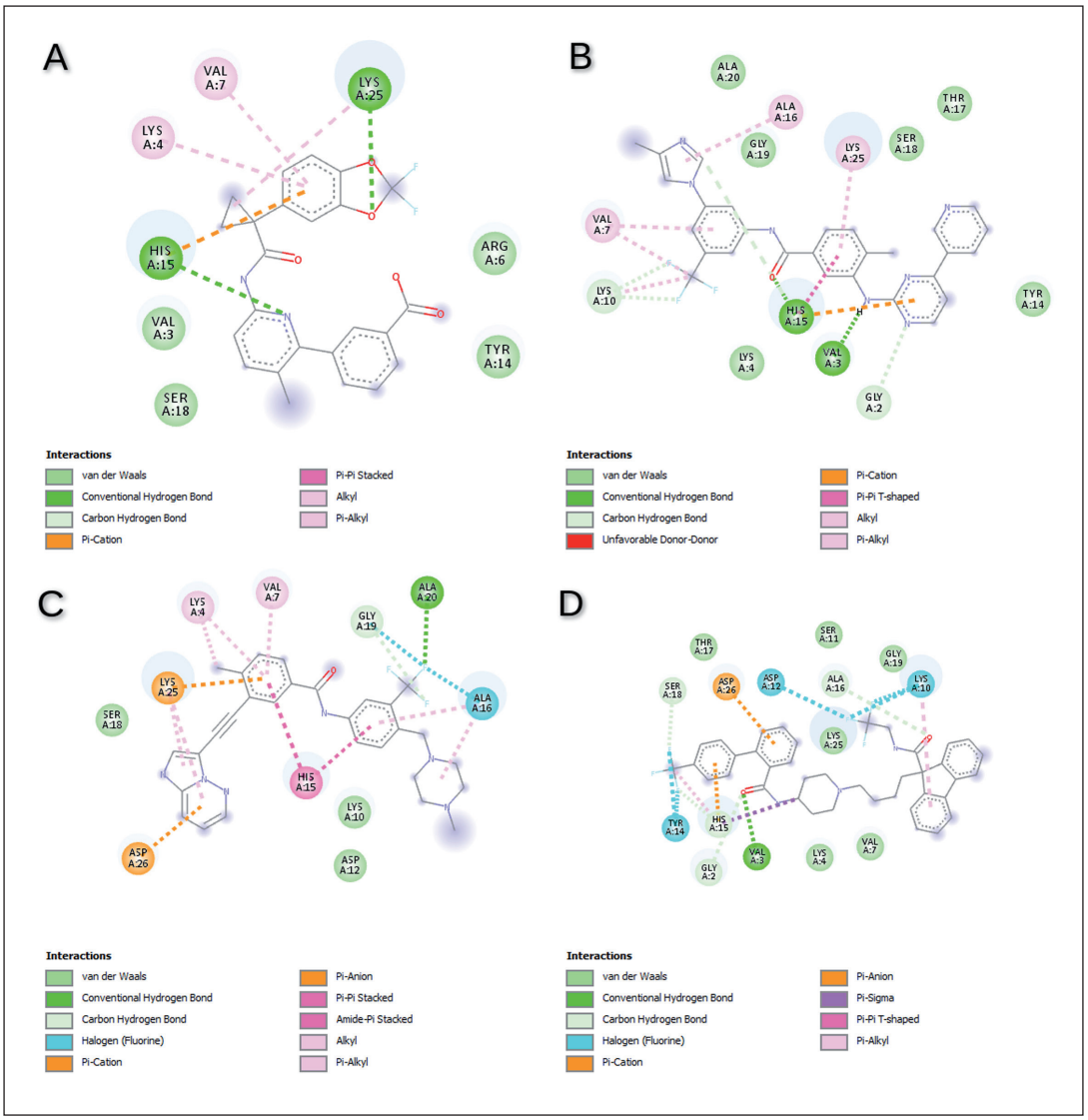

Fig. 2. Selected compounds interactions with Cx43 C-terminal domain. (a) Lumacaftor (b) Nilotinib (c) Ponatinib (d) Lomitapide.

Molecular dynamics simulations

Molecular dynamics simulations are of proven *in silico* methods for obtaining dynamic data at atomic spatial resolution[46,47]. Therefore, the retained compounds were subjected to molecular dynamics simulations for 100 ns to analyze complexes stability.

The root mean square deviation (RMSD) plot is usually used to understand the stability of the complex (Figure 3).

The RMSD represents the deviation of the atomic coordinates of the carbon alpha; a very large value means the structures are different.

The peptide in complex with Nilotinib (blue) showed the most stable RMSD during the 100 ns simulation around 0.4 nm. The Ponatinib complex is also stable around 0.4 nm, but a slight increase was observed after 70 ns simulation while RMSD values for Lumacaftor and Figure 4. Radius of gyration (Rg) plots for Cx43 C-terminal domain (black), Cx43 C-terminal domain-Lomitapide (green), Cx43 C-terminal domain-Ponatinib (red), Cx43 C-terminal domain- Nilotinib (blue) and Cx43 C-terminal domain-Lumacaftor (orange) for 100 ns.

Lomitapide complexes showed high fluctuations that indicate that these complexes undergo conformational changes (Figure 3).

Lomitapide (red), Cx43 C-terminal domain-Ponatinib (green), Cx43 C-terminal domain- Nilotinib (blue) and Cx43 C-terminal domain-Lumacaftor (orange) for 100 ns.

Rg is calculated to determine the compactness of the system during time. Low values indicate more stability while high Rg values explain low

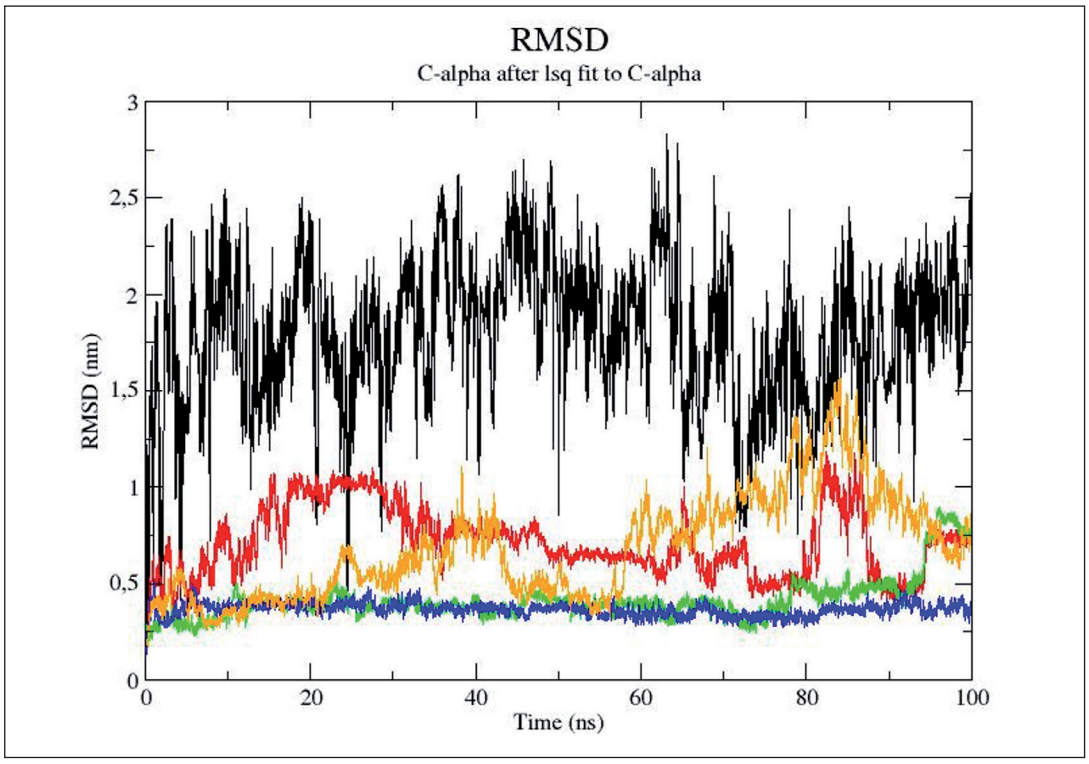

Figure 3. RMSD plots for Cx43 C-terminal domain (black), Cx43 C-terminal domain-Lomitapide (red), Cx43 C-terminal domain-Ponatinib (green), Cx43 C-terminal domain- Nilotinib (blue) and Cx43 C-terminal domain-Lumacaftor (orange) for 100 ns.

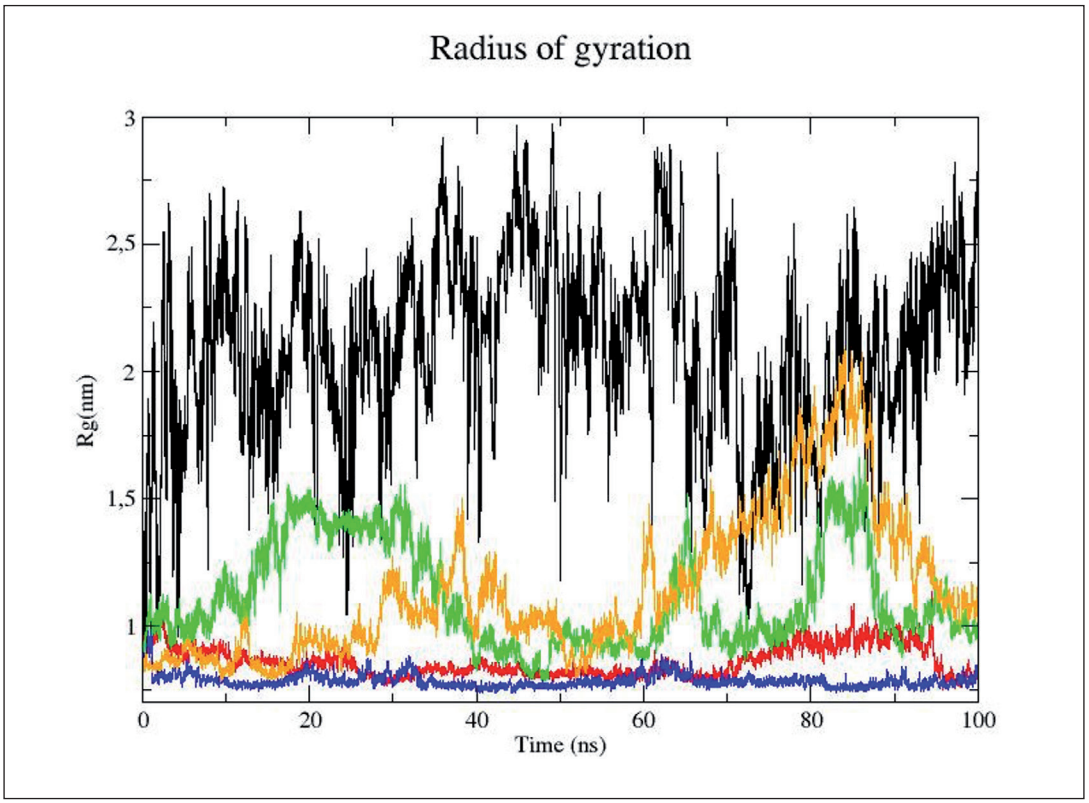

Figure 4. Radius of gyration (Rg) plots for Cx43 C-terminal domain (black), Cx43 C-terminal domain-Lomitapide (green), Cx43 C-terminal domain-Ponatinib (red), Cx43 C-terminal domain- Nilotinib (blue) and Cx43 C-terminal domain-Lumacaftor (orange) for 100 ns.

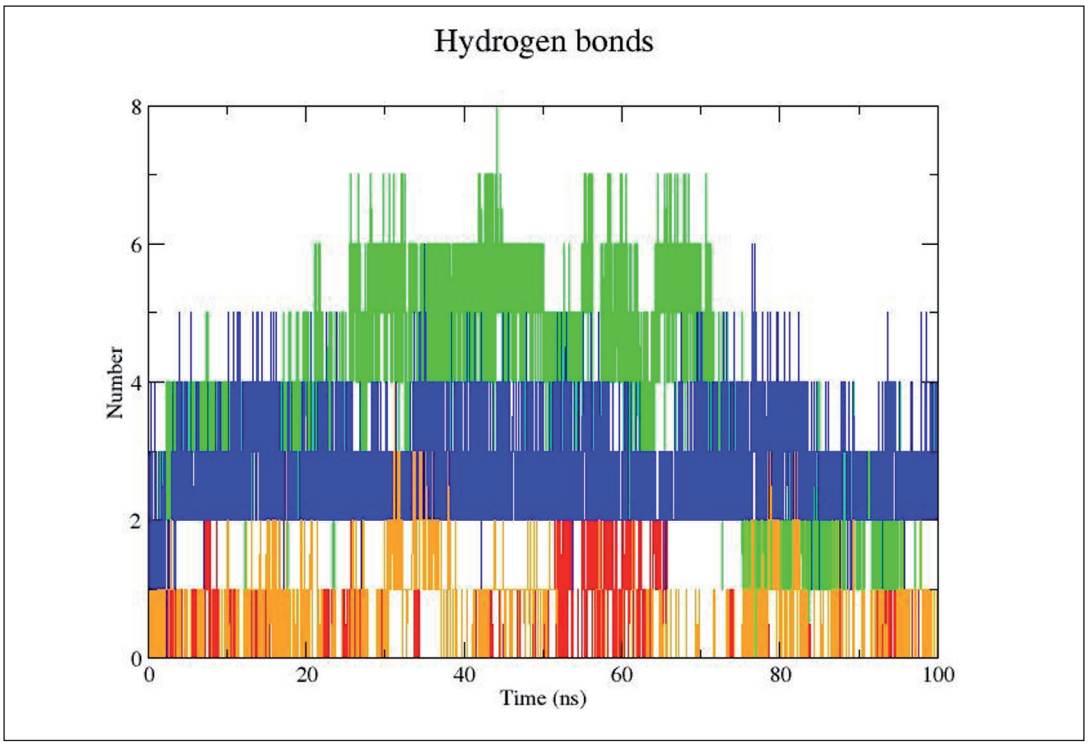

Figure 5. Hydrogen bonds plots for Cx43 C-terminal domain-Lomitapide (red), Cx43 C-terminal domain-Ponatinib (green), Cx43 C-terminal domain- Nilotinib (blue) and Cx43 C-terminal domain-Lumacaftor (orange) for 100 ns.

compactness. As it appears in Figure 4, Lomitapide and Lumacaftor complexes show high Rg values indicating low stability. Ponatinib complex shows higher stability until 65 ns, and higher values are observed till 100 ns revealing less stability. On the other hand, Nilotinib complex reported Rg values (around 0,75 nm) show the higher compactness of the system and, therefore, an increased stability.

Hydrogen bonding plays an essential role in determining the binding strength between compounds and Cx43 C-terminal domain. Nilotinib (blue) has constant range of hydrogen bonds between 2 and 4 in whole simulation, while Ponatinib showed higher number of hydrogen bonds between 25 and 65 ns which significantly decreased between 65 and 100 ns (Figure 5). This is in accordance with observed RMSD changes (Figure 3). The two other complexes showed similar plot patterns with low number of hydrogen bonds along the simulation, which is also in accordance with RMSD Rg plots (Figure 4).

Overall, observations suggested that Cx43 C-terminal domain in complex with Lomitapide and Lumacaftor show poor stability during simulation, while Ponatinib possesses higher stability during the first 65 ns of simulation. Nilotinib complex is clearly the best compound with RMSD and Rg values during the whole simulation and is, therefore, the best candidate as potential drug.

CONCLUSIONS

Connexins and in particular Cx43 are involved in the proliferation and migration of tumor cells. Consequently, these gap junction proteins constitute a potential therapeutic target in the treatment of multiple cancers. By an *in silico* approach, we identified 4 molecules among 1615, approved by the FDA as potential inhibitors of Cx43. In light of molecular docking data and molecular dynamics simulation, Niotinib appears to be the best candidate to target Cx43.

These results pave the way for wider use of Nilotinib. This anticancer drug indicated in the treatment of chronic myeloid leukemia, could be repositioned in the many cancers involving Cx43 and gap junctions.

Acknowledgments:
We are grateful to Dr Merad Hamza Nadjib for his thorough lecture of this article.

Conflict of interest:
The authors declare no conflict of interest.

REFERENCES

1. Laird DW. Life cycle of connexins in health and disease. Biochem J 2006; 394: 527-543.
2. Matsuuchi L, Naus CC. Gap junction proteins on the move: Connexins, the cytoskeleton and migration. Biochem Biophys Acta 2013; 1828: 94-108.

3. Kotini M, Mayorn R. Connexins in migration during development and cancer. Dev Biol 2015; 401: 143-151.
4. Solan JL, Lampe PD. Connexin43 phosphorylation: Structural changes and biological effects. Biochem J 2009; 419: 261–272.
5. Marquez-Rosado L, Solan JL, Dunn CA, Norris RP. Connexin43 phosphorylation in brain, cardiac, endothelial and epithelial tissues. Biochim Biophys Acta 2011; 1818: 1985-1992.
6. Hervé JC. The communicating junctions, composition, structure and characteristics. Biochim Biophys Acta Acta 2012; 1818: 1803-1806.
7. Crespin S, Bechberger J, Mesnil, Naus CC, Sin WC. The carboxy-terminal tail of connexin43 gap junction protein is sufficient to mediate cytoskeleton changes in human glioma cells. J Cell Biochem 2010; 110: 589-597.
8. Ghosh S, Kumar A, Prashad Tripathi R, Chandna S. Connexin-43 regulates p38-mediated cell migration and invasion induced selectively in tumour cells by low doses of γ-radiation in an ERK-1/2-independent manner. Carcinogenesis 2014; 35: 383-395.
9. Sun Q, Wang D, Ai G, Tian L, Zhao L, Chen R., Wang K, Guo D, Yao Y, Liu W, Kong X, Chen X, Zhang Y. Epac1 is involved in cell cycle progression in lung cancer through PKC and Cx43 regulation. Folia Histochem Cytobiol 2018; 56: 21-26.
10. Ye XY, Jiang QH, Hong T, Zhang ZY, Yang RJ, Huang JQ, Hu K, Peng YP. Altered expression of connexin43 and phosphorylation connexin43 in glioma tumors. Int J Clin Exp Pathol 2015; 8: 4296-4306.
11. Zhang A, Hitomi M, Bar-Shain N, Dalimov Z, Ellis L, Velpula KK, Fraizer GC, Gourdie RG, Lathia JD. Connexin 43 expression is associated with increased malignancy in prostate cancer cell lines and functions to promote migration. Oncotarget 2015; 6: 11640-51.
12. Dubina MV, Iatckii NA, Popov DE, Vasil'ev SV, Krutovskikh VA. Connexin 43, but not connexin 32, is mutated at advanced stages of human sporadic colon cancer. Oncogene 2002; 21: 4992-4996.
13. Xu HT, Li QC, Zhang YX, Zhao Y, Liu Y, Yang ZQ, Wang EH. Connexin 43 recruits E-cadherin expression and inhibits the malignant behaviour of lung cancer cells. Folia Histochem Cytobiol 2008; 46: 315-321.
14. Kanczuga-Koda L, Koda M, Sulkowski S, Wincewicz A, Zalewski B, Sulkowska M. Gradual loss of functional gap junction within progression of colorectal cancer - a shift from membranous CX32 and CX43 expression to cytoplasmic pattern during colorectal carcinogenesis. In Vivo 2010; 24: 101-107.
15. Langlois S, Cowan KN, Shao Q, Cowan B J, Laird D W. The tumor-suppressive function of Connexin43 in keratinocytes is mediated in part via interaction with caveolin-1. Cancer Res 2010; 70: 4222-4232.
16. Villares GJ, Zigler M, Bar-Eli M. The emerging role of the thrombin receptor (PAR-1) in melanoma metastasis--a possible therapeutic target. Oncotarget 2011; 2: 8-17.
17. Ryszawy D, Sarna M, Rak M, Szpak K, Kędracka-Krok S, Michalik M, Siedlar M, Zuba-Surma E, Burda K, Korohoda W, Madeja Z, Czyż J. Functional links between Snail-1 and Cx43 account for the recruitment of Cx43-positive cells into the invasive front of prostate cancer. Carcinogenesis 2014; 35: 1920-1930.
18. Grek CL, Rhett JM, Bruce JS, Abt M A, Ghatnekar G S, Yeh ES. Targeting connexin 43 with α-connexin carboxyl-terminal (ACT1) peptide enhances the activity of the targeted inhibitors, tamoxifen and lapatinib, in breast cancer: clinical implication for ACT1. BMC Cancer 2015; 15: 296.
19. Maqbool R, Rashid R, Ismail R, Niaz S, Chowdri NA, Hussain MU. The carboxy-terminal domain of connexin 43 (CT-Cx43) modulates the expression of p53 by altering miR-125b expression in low-grade human breast cancers. Cell Oncol (Dordr) 2015; 38: 443-451.
20. Tabernero A, Gangoso E, Jaraíz-Rodríguez M, Medina JM. The role of connexin43-Src interaction in astrocytomas: A molecular puzzle. Neuroscience 2016; 323: 183-194.
21. Qiu X, Cheng JC, Klausen C, Chang HM, Fan Q, Leung PC. EGF-induced connexin43 negatively regulates cell proliferation in human ovarian cancer. J Cell Physiol 2016; 231: 111-119.
22. Mesnil M. Gap junctions and cancer: implications and perspectives. Med Sci 2004; 20: 197-206.
23. Fu Y, Sun X, Gu Z, Zhuang Z. Connexin 43 Modulates the Cellular Resistance to Paclitaxel via Targeting β-Tubulin in Triple-Negative Breast Cancer. Onco Targets Ther 2020; 13: 5323.
24. Wishart DS, Feunang YD, Guo AC, Lo EJ, Marcu A, Grant JR. Assempour DrugBank 5.0: a major update to the DrugBank database for 2018. Nucleic Acids Res 2018; 46: 1074-1082.
25. Trott O, Olson AJ. AutoDock Vina Improving the speed and accuracy of docking with a new scoring function, efficient optimization and multithreading. J Comput Chem 2010; 31: 455-461.
26. Dallakyan S, Olson AJ. Small-molecule library screening by docking with PyRx. Humana Press 2015; 1263: 243-250.
27. Best R, Zhu X, Shim J, Lopes PEM, Mittal J, Feig M, MacKerell AD. Optimization of the additive charmm all-atom protein force field targeting improved sampling of the backbone **Φ**, **Ψ** and side-chain **X** (1) and **X** (2) dihedral angles. J Chem Theor Comput 2012; 8: 3257-3273.
28. Nosé S. A unified formulation of the constant temperature molecular dynamics methods. J Chem Phys 1984; 81: 511-519.
29. Hoover WG. Canonical dynamics: equilibrium phase-space distributions. Phys Rev 1985; 31: 1695-1697.
30. Parrinello M, Rahman A. Polymorphic transitions in single crystals: a new molecular dynamics method. J Appl Phys 1981; 52: 7182.
31. Saidi Brikci-Nigassa A, Clement MJ, Ha-Duong T, Adjadj E, Ziani L, Pastre D, Curmi PA, Savarin P. Phosphorylation Controls the Interaction of the Connexin43 C-Terminal Domain with Tubulin and Microtubules. Biochemistry 2012; 51: 4331-4342.
32. Talamo Guevara M, McColley SA. The safety of lumacaftor and ivacaftor for the treatment of cystic fibrosis. Expert Opin Drug Saf 2017; 16: 1305-1311.
33. Deeks ED. Lumacaftor/Ivacaftor: A Review in Cystic Fibrosis. Drugs 2016; 76: 1191-1220.
34. Connett GJ. Lumacaftor-ivacaftor in the treatment of cystic fibrosis: design, development and place in therapy. Drug Des Devel Ther 2019; 13: 2405-2412.
35. Cuchel M, Meagher EA, Du Toit Theron H, Blom DJ, Marais AD, Hegele RA, Averna MR, Sirtori CR, Shah PK, Gaudet D, Stefanutti C, Vigna GB, Du Plessis AM, Propert KJ, Sasiela WJ, Bloedon LT, Rader DJ. Efficacy and safety of a microsomal triglyceride transfer protein inhibitor in patients with homozygous familial hypercholesterolaemia: a single-arm, open-label, phase 3 study. Lancet 2013; 381: 40-46.
36. Yin W, Mao C, Luan X, Shen DD, Shen Q, Su H, Wang X, Zhou F, Zhao W, Gao M, Chang S, Xie YC, Tian G, Jiang HW, Tao SC, Shen J, Jiang Y, Jiang H, Xu Y, Zhang S, Zhang Y, Xu H E. Structural basis for inhibition of the RNA-dependent RNA polymerase from SARS-CoV-2 by remdesivir. Science 2020; 368: 1499-1504.

37. Yasu T, Momo K, Kobayashi S, Kuroda S, Tojo A. Simple determination of plasma ponatinib concentration using HPLC. Biol Pharm Bull 2018; 41: 254-258.
38. Haouala A, Widmer N, Duchosal MA, Montemurro M, Buclin T, Decosterd LA. Drug interactions with the tyrosine kinase inhibitors imatinib, dasatinib, and nilotinib. Blood 2011; 117: 75-87.
39. Price KE, Saleem N, Lee G, Steinberg M. Potential of ponatinib to treat chronic myeloid leukemia and acute lymphoblastic leukemia. Onco Targets Ther 2013; 6: 1111-1118.
40. Lunghi M, Patriarca A, Greco M, Taherinasab A, Della Starza I, Cavalli M, Gaidano G, Foà R, Chiaretti S. Ponatinib for the treatment of Ph-like acute lymphoblastic leukemia. Leuk Lymphoma 2021; 62: 755-757.
41. Cortes JE, Kim DW, Pinilla-Ibarz J, Le Coutre PD, Paquette R, Chuah C, Nicolini FE, Apperley JF, Khoury HJ, Talpaz M, DeAngelo DJ, Abruzzese E, Rea D, Baccarani M, Müller MC, Gambacorti-Passerini C, Lustgarten S, Rivera VM, Haluska FG, Guilhot F, Deininger MW, Hochhaus A, Hughes TP, Shah NP, Kantarjian HM. Ponatinib efficacy and safety in Philadelphia chromosome-positive leukemia: final 5-year results of the phase 2 PACE trial. Blood 2018; 132: 393-404.
42. Massaro F, Molica M, Breccia M. Ponatinib: a review of efficacy and safety. Curr Cancer Drug Targets 2018; 18: 847-856.
43. Tan P, He L, Xing C, Mao J, Yu X, Zhu M, Diao L, Han L, Zhou Y, You MJ, Wang HY, Wang RF. Myeloid loss of Beclin 1 promotes PD-L1hi precursor B cell lymphoma development. J Clin Invest 2019; 129: 5261-5277.
44. Pagan FL, Hebron ML, Wilmarth B, Torres-Yaghi Y, Lawler A, Mundel EE, Yusuf N, Starr NJ, Anjum M, Arellano J, Howard HH, Shi W, Mulki S, Kurd-Misto T, Matar S, Liu X, Ahn J, Moussa C. Nilotinib Effects on Safety, Tolerability, and Potential Biomarkers in Parkinson Disease: A Phase 2 Randomized Clinical Trial. JAMA Neurol 2020; 77: 309-317.
45. Sacha T, Saglio G. Nilotinib in the treatment of chronic myeloid leukemia. Future Oncol 2018; 15: 953-965.
46. Benson NC, Daggett V. A comparison of multiscale methods for the analysis of molecular dynamics simulations. J Phys Chem B 2012; 116: 8722-8731.
47. Kumar A, Choudhir G, Shukla SK, Sharma M, Tyagi P, Bhushan A, Rathore M. Identification of phytochemical inhibitors against main protease of COVID-19 using molecular modeling approaches. J Biomol Struct Dyn 2021; 39: 3760-3770.